FD-SOI mm-Wave Differential Single-Pole Switches with Ultra-High Isolation

Martin Rack, Lucas Nyssens, Sidina Wane*, Damienne Bajon*, Dimitri Lederer, Jean-Pierre Raskin

Université catholique de Louvain, Belgium
*eV-Technologies, France
E-mail: martin.rack@uclouvain.be

2021 International Symposium on VLSI Technology, Systems and Applications (VLSI-TSA) | 978-1-6654-1934-5/20/$31.00 ©2021 IEEE | DOI: 10.1109/VLSI-TSA51926.2021.9440095

ABSTRACT

FD-SOI is a promising technology for integrating mm-wave front-end circuitry. In this paper, fully-differential SPST and SP4T switches are designed with wideband operation (DC up to 50 GHz) using GlobalFoundries' 22FDX® platform. Based on a differential mode-blocking topology, the switches can achieve isolations better than 50 dB. At 28 GHz, the balanced topology achieves an insertion loss of 1.92 dB, a 1-dB compression of 23.5 dBm and an IIP3 of 47.6 dBm.

HIGH-ISOLATION DIFFERENTIAL TOPOLOGY

The differential mode blocking topology is presented in Figure 1. This X-SPST topology was first developed in [1]. When a differential input signal is applied between nodes a_1 and a_2, the differential output signal (between nodes b_1 and b_2) is perfectly equal to zero if the four branch impedances are equal. Let branches 1 and 2 be the *direct branches* (D) of admittance Y_D, and branches 3 and 4 be the *crossed branches* (X) of admittance Y_X. The differential Y_{21} admittance parameter of this topology is then: $Y_{21} = (Y_X - Y_D)/2$.

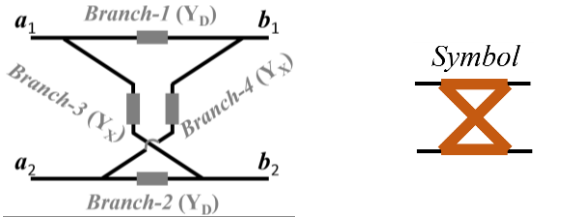


FIGURE 1. LEFT: Topology of the X-SPST. RIGHT: Symbol.

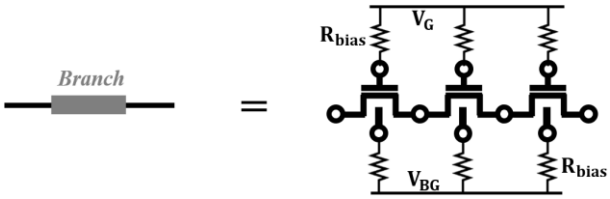


FIGURE 2. Implementing each branch impedance with stacked FETs.

Each branch impedance is implemented using a series stack of three 22FDX® SLVT NFETs (with 20 nm gate length), as depicted by Figure 2, targeting above 20 dBm of power handling [2].

In the ON state, branches 1 and 2 are turned on by applying a front gate bias of V_g = 0.9 V and a back-gate bias of V_{bg} = 3 V while branches 3 and 4 are turned off with V_g = -0.9 V and V_{bg} = 0 V. In that case $Y_{D\text{-}ON}$ is high and $Y_{X\text{-}OFF}$ is low and $Y_{21\text{-}ON}$ reduces to $-Y_{D\text{-}ON}/2$.

In the OFF state, all branches are turned off. Then, $Y_{21\text{-}OFF}$ becomes $(Y_{X\text{-}OFF} - Y_{D\text{-}OFF})/2$. If the branch impedances are equal, destructive interference occurs between the signal passed through the D branches and the anti-phase signal passed through the X branches, and $Y_{21} = 0$.

MEASUREMENT RESULTS

Two types of X-SPST and an X-SP4T were designed and fabricated, with diagrams and photographs given in Figure 3. All FETs implement finger widths of W_f = 3 µm. The total width of a FET is given by $W_{tot} = W_f N_f$, where the number of fingers in the D and X branches ($N_{f\text{-}D}$ and $N_{f\text{-}X}$) will be different for each considered switch.

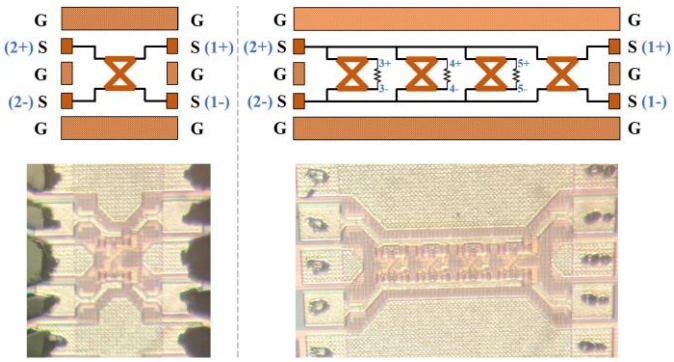


FIGURE 3. Diagrams and microscope photos of the X-switches.

All measured differential mode parameters S_{ijdd} presented have undergone an open deembedding of the RF measurement pads. Figure 4 plots the measured differential insertion loss ($IL = -S_{21\text{-}ON}$ [dB]) and isolation ($ISO = -S_{21\text{-}OFF}$ [dB]) of the three fabricated switches.

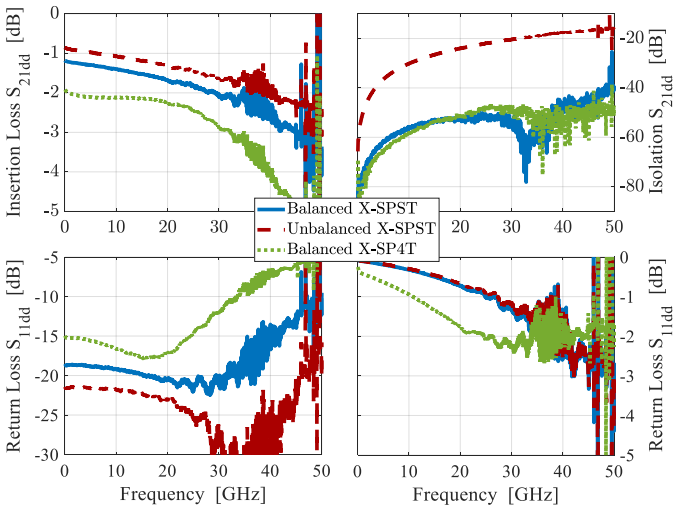


FIGURE 4. Differential mode S_{ijdd} parameters of the X-SPkTs.

Balanced X-SPST

In the balanced topology the D and X branches are designed as identical with $N_{f\text{-}D} = N_{f\text{-}X} = 35$. Then, $Y_{21\text{-}OFF}$ is theoretically equal to zero as $Y_{X\text{-}OFF}$ and $Y_{D\text{-}OFF}$ are equal. Figure 4 shows that the balanced X-SPST switch presents very high isolation to the differential input, achieving -53 dB at 28 GHz. The design was performed to minimize IL and at 28 GHz an IL of 1.92 dB is achieved when the D branches are ON and the X branches are OFF (in that case $Y_{21} = -Y_{D\text{-}ON}/2$). The IL remains lower than 3 dB up to roughly 50 GHz.

An optimum sizing of the FETs exists as is depicted in Figure 5 (left), where the $N_f = N_{f\text{-}D} = N_{f\text{-}X}$ parameter is swept and the ON-state IL and return loss ($RL = -S_{11\text{-}ON}$) are plotted. The ON-state D branches pass the differential signal to the output, while the OFF-state X

Authorized licensed use limited to: Univ Catholique de Louvain/UCL. Downloaded on September 01,2021 at 10:17:19 UTC from IEEE Xplore. Restrictions apply.

branches will couple the anti-phase signal to the output. For low FET widths the $Y_{D\text{-}ON}$ (= $1/R_{ON}$) parameters are too low, and IL is degraded due to the lossy resistive FETs. For high values of N_f the $Y_{X\text{-}OFF}$ (= $j\omega C_{OFF}$) parameters are responsible for significant parasitics that degrades IL and RL simultaneously by contributing to destructive interference at the differential output. Figure 5 (left) shows that an IL optimum lies between $N_f = 35$ and $N_f = 45$. The value of 35 was chosen in this work in order to facilitate good matching of the overall layout.

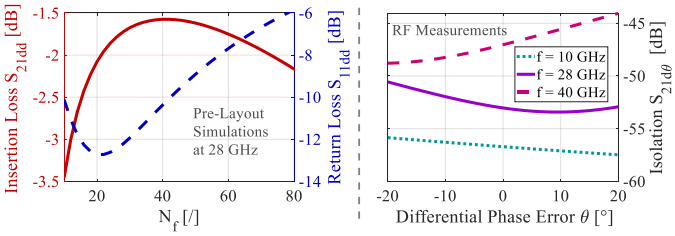


FIGURE 5. LEFT: Optimal FET width for lowest IL (pre-layout sim.). RIGHT: Isolation $S_{21d\theta}$ of the balanced X-SPST vs. input phase error.

Unbalanced X-SPST

It may not be necessary to achieve more than 20 dB of isolation, and, in that case, the topology can be purposefully unbalanced ($N_{f\text{-}D} \neq N_{f\text{-}X}$) to reduce IL. A design was performed to minimize IL while ensuring 20 dB isolation at 28 GHz, and this was achieved for $N_{f\text{-}D} = 50$ and $N_{f\text{-}X} = 12$. Figure 4 then plots the IL of this unbalanced X-SPST design which achieves a value of 1.55 dB at 28 GHz. The isolation spec is well met, as Figure 3 shows that ISO(28 GHz) = 21 dB. The isolation limits the frequency operation range of this switch, as above 35 GHz it is considered too poor a specification.

Balanced X-SP4T

The balanced X-SP4T device is composed of four balanced X-SPST unit cells (see Figure 3). When the pole of the switch establishes an ON state with one of the four throws, the three OFF state SPST cells contribute to shunt parasitics. For this reason, in the design of any SPkT device, the optimum size of the unit SPST cell is different for each k. For our X-SP4T the optimal cell was sized by $N_{f\text{-}D} = N_{f\text{-}X} = 21$.

The full X-SP4T device is characterized using two differential RF ports, and the other switch ports are emulated on chip using three precision 50 Ω resistors (see Figure 3). In the ON state the device exhibits 2.65 dB of IL at 28 GHz, while the balanced topology ensures excellent isolation in the OFF state, which is 48.5 dB at 28 GHz. The IL rolls off by 2 dB at 40 GHz, and IL(40 GHz) = 4 dB.

Switch Return Loss

In the ON state, Figure 4 shows that the devices are well matched, with a return loss (RL = $-S_{11}$ [dB]) better than 10 dB over the three switch's operation ranges. At 28 GHz, RL is 15 to 25 dB.

In the OFF state, the RL is high, as the switch topology is of a reflective nature (rather than absorptive).

Input Differential Phase Error

In a practical IC, a differential phase error θ may arise at the device's input (different electrical phase length of the two feed paths towards the device, imperfect balun, etc.). It is then pertinent to study the isolation as a function of θ, i.e. node a_1 is excited by $+a \cdot e^{j\theta}$ while node a_2 is excited by -a. In that case, the $S_{21d\theta}$ coupling parameter from this input signal to the differential output is plotted in Figure 5 at several frequencies.

A fairly week dependency is observed, demonstrating a good isolation robustness with respect to an input differential phase error up to ±20°. A similar analysis was performed in [3].

Large-Signal Performance

The devices were simulated under large-signal with a dual tone differential input at 28 GHz and 28.1 GHz, whose powers were simultaneously swept up to 25 dBm. From the fundamental output powers and the third intermodulation product output power (at 28.2 GHz) the 1-dB compression point P1dB and input third order intercept point IIP3 were extracted. Given in Table 1 for the three fabricated devices, they are in the range of 24 dBm and 50 dBm, respectively.

CONCLUSION

The design of fully-differential SPST and SP4T switches with ultra-high isolation enabled by a mode-blocking topology was presented in this paper, implemented in 22 nm FD-SOI. A benchmarking review (Table 1) reveals that these wideband mm-wave switches are at the state-of-the-art at 28 GHz, in terms of insertion loss (measured 1.92 dB), isolation (measured 53 dB), P1dB (simulated 23.5 dBm) and IIP3 (simulated 47.6 dBm) for the balanced design.

ACKNOWLEDGEMENT

We thank GLOBALFOUNDRIES for chip fabrication and support.

REFERENCES

[1] H. Erkens and H. Heuermann, *IEEE Trans. on Microw. Theory and Techniques*, vol. 54, no. 6, pp. 2376-2382, June 2006.

[2] M. Rack *et al*., *2020 IEEE Radio Frequency Integrated Circuits Symposium (RFIC)*, Los Angeles, CA, USA, 2020, pp. 67-70.

[3] A. Eltaliawy, J. R. Long and N. Cahoon, *2020 IEEE Radio Frequency Integrated Circuits Symposium (RFIC)*, Los Angeles, CA, USA, 2020, pp. 63-66.

[4] B. Yu *et al*., *IEEE Transactions on Microwave Theory and Techniques*, vol. 65, no. 10, pp. 3937-3949, Oct. 2017.

[5] C. Li *et al*., *2018 IEEE 18th Top. Meet. on Silic. Monolith. Integrat. Circ. in RF Syst. (SiRF)*, Anaheim, CA, 2018, pp. 1-3.

[6] A. Balasubramaniyan and A. Bellaouar, *2018 IEEE SOI-3D-Subthreshold Microelectronics Technology Unified Conference (S3S)*, Burlingame, CA, USA, 2018, pp. 1-2.

TABLE 1. State-of-the-art mm-wave switch modules in SOI technology.

Simulated data	[4] 2017	[5] 2017	[6] 2018	[2] 2020	[3] 2020	This Work 2021		
Techno	130nm SOI	45-RFSOI	22FDX®	22FDX®	45-RFSOI	22FDX®		
Type	SPDT Single-Ended	SPDT Single-Ended	SPST Single-Ended	SPDT Single-Ended	SPST Differential	SPST Differential		SP4T Differential
Topology	Series-Shunt with matching	Series-Shunt	Series-Shunt	Series-Shunt with matching	X-balanced	X-unbalanced	X-balanced	
Band	DC-50	DC-50	DC-40	DC-40	DC-43	DC-35	DC-50	DC-40
IL(28 GHz) [dB]	1.0	0.7	1.1	1.66	2.5	1.55	1.92	2.65
ISO(28 GHz) [dB]	32	24	24	33.4	57	21	53	48.5
P1dB [dBm]	14	29.5	23	20.5	19.6	24.9*	23.5*	23.2*
IIP3 [dBm]	27	46	43	38.5	25.5	52.2*	47.6*	42.2*
Device Size [10^{-3} mm²]	40	4	/	34	5.8	7.1	7.1	35

Authorized licensed use limited to: Univ Catholique de Louvain/UCL. Downloaded on September 01,2021 at 10:17:19 UTC from IEEE Xplore. Restrictions apply.